HHS Public Access

Author manuscript

Mol Cell. Author manuscript; available in PMC 2017 April 21.

Published in final edited form as:

Mol Cell. 2016 April 21; 62(2): 260–271. doi:10.1016/j.molcel.2016.04.005.

Molecular Mechanism of Protein Kinase Recognition and Sorting by the Hsp90 Kinome-Specific Cochaperone Cdc37

Dimitra Keramisanou[1], **Adam Aboalroub**[1], **Ziming Zhang**[1], **Wenjun Liu**[2], **Devon Marshall**[1], **Andrea Diviney**[1], **Randy W. Larsen**[1], **Ralf Landgraf**[2,3], and **Ioannis Gelis**[1,*]

[1]Department of Chemistry, University of South Florida, Tampa, FL 33620, USA

[2]Department of Biochemistry and Molecular Biology, Miller School of Medicine, University of Miami, Miami, FL 33136, USA

[3]Sylvester Comprehensive Cancer Center, Miller School of Medicine, University of Miami, Miami, FL 33136, USA

SUMMARY

Despite the essential functions of Hsp90, little is known about the mechanism that controls substrate entry into its chaperone cycle. We show that the role of Cdc37 cochaperone reaches beyond that of an adaptor protein and find that it participates in the selective recruitment of only client kinases. Cdc37 recognizes kinase specificity determinants in both clients and nonclients and acts as a general kinase scanning factor. Kinase sorting within the client-to-nonclient continuum relies on the ability of Cdc37 to challenge the conformational stability of clients by locally unfolding them. This metastable conformational state has high affinity for Cdc37 and forms stable complexes through a multidomain cochaperone interface. The interaction with nonclients is not accompanied by conformational changes of the substrate and results in substrate dissociation. Collectively, Cdc37 performs a quality control of protein kinases, where induced conformational instability acts as a "flag" for Hsp90 dependence and stable cochaperone association.

Graphical Abstract

*Correspondence: igelis@usf.edu.

AUTHOR CONTRIBUTIONS

D.K. and I.G. designed the research; all authors contributed in performing the research; D.K., A.A., W.L., Z.Z., R.W.L., R.L., and I.G. analyzed data; I.G. wrote the manuscript.

ACCESSION NUMBERS

The coordinates for the structural model of N-Cdc37 have been deposited in the Protein Data Bank under ID code PDB: 2NCA, and the assignments have been deposited at BMRB under ID code BMRB: 26012.

SUPPLEMENTAL INFORMATION

Supplemental Information includes Supplemental Experimental Procedures, seven figures, and one table and can be found with this article online at http://dx.doi.org/10.1016/j.molcel.2016.04.005.

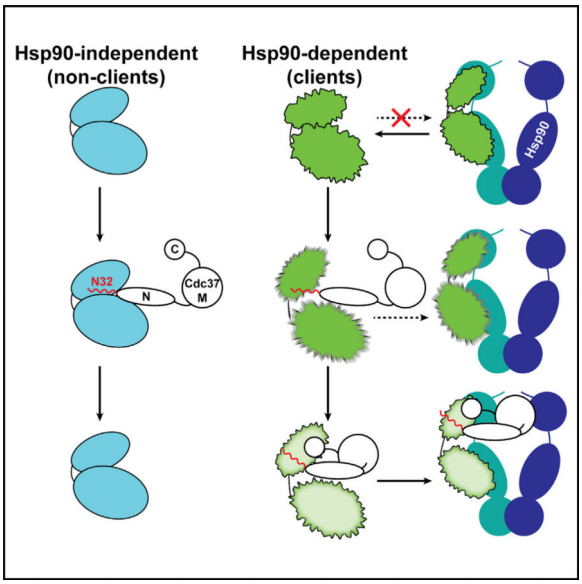

INTRODUCTION

Selective entry into the Hsp90 chaperone cycle is a critical step in proteostasis and regulation of signaling pathways. The process is challenged by the lack of sequence and structural homology between the substrates, termed clients (Taipale et al., 2010), and thus, Hsp90 has acquired recruiter cochaperones to gain the essential specificity elements (Röhl et al., 2013). Cdc37 is the ubiquitous cochaperone of the machinery controlling the entry of a large and diverse gamut of protein kinases (Caplan et al., 2007; Karnitz and Felts, 2007; Taipale et al., 2012). As with other recruiter cochaperones, the mechanisms of substrate recognition and sorting within the client-nonclient continuum remain elusive.

There is the consensus that the first 40 residues of Cdc37, which exhibit the highest sequence homology, contain residues critical for conferring kinase specificity. A construct lacking the first 30 residues (Δ30-Cdc37) does not associate with bRaf and cannot compete with ATP for kinase binding (Polier et al., 2013), while deletion of residues 26–38 results in impaired signaling by the sevenless receptor (Cutforth and Rubin, 1994). Association with HRI is abolished by either of the Y4A or W7A mutations, and is significantly affected by the V2A and D3A mutations (Shao et al., 2003a). Y4 phosphorylation abolishes association with a certain class of kinases (Xu et al., 2012), while S13 phosphorylation promotes formation of stable Hsp90-Cdc37-kinase ternary complexes, without affecting the stability of binary Cdc37-kinase complexes (Miyata and Nishida, 2004; Polier et al., 2013; Shao et al., 2003b; Vaughan et al., 2008). However, two regions outside the N-terminal domain (N-Cdc37) were identified to regulate kinase binding, making the kinase recognition site a matter of controversy. A 20 amino acid stretch (181–200) in the middle domain (M-Cdc37) was proposed to comprise the recognition site for cRaf (Terasawa and Minami, 2005), and either Y298 phosphorylation (Xu et al., 2012) or the W342C mutation (Cutforth and Rubin, 1994) has a detrimental effect on kinase binding, implicating the previously uncharacterized C-terminal domain (C-Cdc37) in kinase binding. In this respect, it was also shown that C-

terminal constructs interact with bRaf in the presence of the full-length protein (Eckl et al., 2015).

On the kinase side, the catalytic domain is unambiguously implicated in the interaction with the Hsp90 machinery (Vaughan et al., 2006). Although kinase primary sequence elements and surface characteristics have been proposed as Hsp90-client-specificity determinants (Citri et al., 2006; Prince and Matts, 2004; Scroggins et al., 2003; Xu et al., 2005), these features cannot account for the striking selectivity between highly homologous kinases such as v-Src and c-Src (Xu and Lindquist, 1993; Xu et al., 1999). Moreover, the sequence and structural diversity of Hsp90-dependent proteins suggests that such “motifs” do not exist. Instead, the current paradigm suggests that the machinery sorts kinases within the strong-to-nonclient continuum by sensing their thermal stability (Boczek et al., 2015; Taipale et al., 2012, 2013), and specificity determinants on the kinase are recognized by Cdc37, which recruits the substrate to Hsp90. These Cdc37 recognition sites reside at the conserved glycine-rich motif and the loop connecting the αC-helix to the β4-strand (Prince and Matts, 2004; Zhao et al., 2004). The observed Cdc37 inhibition of nucleotide binding to the kinase domain reinforces the notion that Cdc37 recognizes sequence or structural features in the vicinity of the ATP-binding cleft (Polier et al., 2013).

Currently, the molecular mechanism of kinase recognition and the role of Cdc37 in sensing the thermal stability of a kinase domain remain unknown. Here we show that Cdc37 recognizes kinases through a staged process that affords kinase specificity and client selectivity to the Hsp90 chaperone machinery. N-Cdc37 acts as a kinase scanning factor with broad kinase specificity, recognizing both clients and nonclients. Client selectivity resides in the ability of N-Cdc37 to induce local unfolding only to client kinases and promote stable association through C-Cdc37. Interaction with nonclients does not alter their conformational properties, and the substrate dissociates. Thus, Cdc37 senses the thermal stability of kinase domains by subjecting them to a controlled stress test of conformational stability.

RESULTS

Conformational Properties of N-Cdc37

To understand the role of N-Cdc37 in recruiting protein kinases to Hsp90, we first characterized its structural and dynamic properties using NMR spectroscopy. The ^{1}H-^{15}N HSQC spectrum of N-Cdc37 exhibits a large dynamic range of signal intensities and limited signal dispersion (Sreeramulu et al., 2009a, 2009b) (Figure 1A). Secondary structure prediction, using backbone chemical shifts, indicates that one-third of N-Cdc37 acquires a coil conformation, including the highly conserved 25 N-terminal amino acids and the extreme 16 C-terminal amino acids (Figure 1B). The rest of the domain forms two helices (α_1 and α_2) connected through a loop (aa 73–77) (Figure 1B). Phosphorylation of N-Cdc37 at S13 does not affect the boundaries of the predicted secondary structure elements (Figures S1A–S1C, available online). In addition, $\{^{1}H\}$-^{15}N heteronuclear NOEs (hNOEs) provide direct evidence that N-Cdc37 exhibits differential flexibility (Figure 1C). Residues in the predicted helices α_1 and α_2 exhibit hNOEs near 0.8, indicating that internal dynamics faster than the overall domain tumbling are not present. In contrast, the terminal regions (aa 1–25

and 115–126) exhibit low (<0.3) or even negative hNOEs, suggesting that ps-ns dynamics are operative and ample backbone conformational heterogeneity is present for these regions.

Although the ^{1}H-^{15}N HSQC for N-Cdc37 is 93% complete, assignment of sidechain proton signals for most residues in α_1 and α_2 was hindered by extensive signal overlap, conformational exchange, and/or a fully anisotropic motion. To obtain structural information, we adopted an alternative approach and relied on CH_3-derived long-range NOEs. An adequate number of inter-helical CH_3-CH_3 long-range NOEs, as well as many medium- and short-range CH_3-CH_3, HN-CH_3, and HN-HN NOEs, allowed us to define the fold of the domain at a resolution suitable for functional studies (Figures S1D and S1E; Supplemental Information). The central region, comprised of helices α_1 and α_2, forms a U-shaped, antiparallel two-helix bundle, while the absence of any long-range NOE for the N- and C-tails suggests that these regions are indeed flexible (Figure 1D). The interface of the bundle is lined with clusters of highly conserved hydrophobic residues, but the lack of a regular coiled-coil repeat pitch results in a loosely packed structure (Figure 1E). Comparison of the ^{1}H-^{15}N HSQC spectra of N-Cdc37 and Cdc37 confirms that the fold is the same in the context of the full-length protein, as previously suggested (Sreeramulu et al., 2009b) (Figure S1F).

In summary, N-Cdc37 forms an independently folded domain that adopts a two-helix bundle conformation and displays differential dynamics containing long N- and C-terminal flexible tails.

Interaction of Cdc37 with the Client Kinase bRaf

As a model kinase domain, we used an engineered form of bRaf with significantly weak self-association properties and increased solubility (Thevakumaran et al., 2015; Tsai et al., 2008). bRaf is a well-characterized Hsp90 client (da Rocha Dias et al., 2005; Grbovic et al., 2006; Taipale et al., 2012; Vaughan et al., 2006), and this variant accurately recapitulates binary Cdc37-bRaf and ternary Hsp90-Cdc37-bRaf complexes formed by the wild-type bRaf kinase domain in vivo (Polier et al., 2013). To assess the oligomeric state and the stoichiometry of in vitro-assembled binary complexes, we characterized the hydrodynamic properties of Cdc37, bRaf, and Cdc37-bRaf at different molar ratios (Figure 2A). For all three species, the molar mass distribution determined by analytical size-exclusion chromatography coupled to multiangle light scattering detection (SEC-MALS) is in agreement with a model where Cdc37 and bRaf are monomeric in their free state and form a complex with a 1:1 stoichiometry (Sreeramulu et al., 2009b).

To obtain site-specific information on Cdc37 elements mediating stable association with client kinases, we used the methyl-TROSY approach (Figure 3) and followed changes in the ^{1}H-^{13}C HMQC spectra of Cdc37 as a function of increasing amounts of unlabeled bRaf. Addition of bRaf at a molar ratio of 1:1 affects the position and linewidth of Cdc37 signals from different domains in two distinct ways (Figures 2B and S2A). Signals from N- and C-Cdc37 disappear and a new set of signals appears at different positions, without any significant change in linewidths, suggesting that complex formation occurs at a slow exchange regime ($k_{ex} << |\Delta\nu|$), as expected for a complex with a K_d of 0.2 μM (Polier et al., 2013). However, signals from M-Cdc37 show extreme broadening and disappear or split into

two broad signals of almost equal intensity, one for each of the free and bRaf-bound states (Figure S2B).

Analysis of chemical shift perturbations (CSPs) reveals that the most prominent changes (greater than one SD from the mean, i.e., $\Delta\delta > 0.13$ ppm) occur at C-Cdc37 (Figure 2C) and include L301, L317, I321, M333, and I337. With the exception of L301 (located at the α_1-α_2 linker), L317, I321, M333, and M337 belong to helices α_3 and α_4 of C-Cdc37. Other signals that become affected include those of V314 (broadened beyond detection), as well as those of L297, V311, M316, A329, and V343 (CSP greater than the mean, i.e., $\Delta\delta > 0.028$ ppm). When this subset of residues is mapped on the structure of C-Cdc37, a discrete and highly conserved hydrophobic patch is formed, suggesting that kinase binding to this domain is localized at this region (Figures 2D and S2C). The N-Cdc37 signals that experience significant CSP include V6, I10, A26, L28, A35, V37, M40, M105, and M112, while the signal of I23 broadens beyond detection. This observation provides direct evidence that N-Cdc37 residues beyond the N terminus are involved in kinase binding (Figure 2E). On the other hand, the effect of bRaf addition on M-Cdc37 signals cannot be accounted for by a direct interaction. The observed 1:1 stoichiometry (Figure 2A) (Polier et al., 2013) and the pattern of signal intensity changes during the course of the titration (Figure S2D) suggest that the source of M-Cdc37 signal splitting is not formation of an asymmetric complex between dimeric Cdc37 and monomeric bRaf. Furthermore, under this set of experimental conditions the observed signal broadening, which results in an ~70% signal attenuation, cannot be due to chemical exchange caused by bRaf binding or transient self-association of the Cdc37-bRaf complex to form a symmetric 2:2 complex (Figure S2E). Therefore, the interaction of N- and C-Cdc37 with bRaf affects the conformational properties of M-Cdc37 by inducing exchange to an alternate conformational state (changes in chemical shift) at an intermediate/slow timescale (severe line broadening). Significant CSP is observed in the vicinity of the Hsp90 binding site, including the signals of M164 and L205, which are critical for stabilizing the Cdc37-Hsp90 complex (Figure S2F) (Roe et al., 2004; Smith et al., 2015; Sreeramulu et al., 2009b). Thus, kinase binding to N- and C-Cdc37 is transmitted to M-Cdc37, in a manner that may modulate the Cdc37-Hsp90 interaction and allow for the coordinated binding and release of the cochaperone during the Hsp90 chaperone cycle.

We also examined whether S13 phosphorylation alters the mode of Cdc37-bRaf recognition. Addition of bRaf to phosphorylated or nonphosphorylated Cdc37 produces identical changes to the ^{1}H-^{13}C-HMQC maps, with C-Cdc37 signals exhibiting the largest CSP and signals from N-Cdc37 showing exactly the same pattern. In addition, the two forms produce identical thermodynamic signatures of binding and have the same affinity for bRaf (Figure S3). Therefore, S13 phosphorylation does not impact the mode of recognition or affinity for protein kinases. This is in agreement with the hypothesis that CK2 phosphorylation regulates the chaperone cycle at a stage later than Cdc37 recognition and is required for stabilizing ternary Hsp90-Cdc37-kinase complexes (Polier et al., 2013; Vaughan et al., 2008).

In summary, Cdc37 associates with a client kinase to form a stable complex of 1:1 stoichiometry. The methyl-TROSY approach provides direct evidence for an unprecedented synergy between N- and C-Cdc37 and reveals that residues beyond the extreme N terminus

of N-Cdc37, together with a conserved hydrophobic patch on C-Cdc37, participate in binding.

Mutations in C-Cdc37 Compromise the Interaction of Cdc37 with Clients

To further characterize the C-Cdc37 client binding site, we investigated the impact of helix α_3 mutants on complexes of Cdc37 with bRaf (wild-type or V600E, bRaf^{V600E}) and the receptor tyrosine kinase ErbB2 in human MCF7 cells. M316, L317, and I321 were altered to produce two double mutants, M316A/L317A and M316A/L317E (denoted AA and AE), and two triple mutants, M316A/L317A/I321A and M316A/L317E/I321E (denoted AAA and AEE). At comparable coexpression of biotin-tagged bRaf, the ratio of biotinylated bRaf to recovered Cdc37 drops by >90% for all four mutants (Figure 4A) (>80% adjusted for biotinylation yield). Compared to bRaf, the effect of Cdc37 mutations is more profound on the synthesis yield of the membrane-localized ErbB2 receptor, reflecting the more complex maturation path and additional levels of quality control (Figure 4B). For equivalent amounts of biotinylated ErbB2, the recovery of associated Cdc37 drops sharply for all four mutants. Hence, both clients reveal a similar and very pronounced sensitivity in their client-Cdc37 complex recovery, despite large differences in their mode of processing and sensitivity of production rates toward Cdc37 defects.

Because the AEE mutant shows consistent impaired interaction for both clients, it was further evaluated for its impact on the interaction with wild-type and bRaf^{V600E} (Figure 4C). Consistent with published reports, the interaction of Cdc37 with bRaf^{V600E} is significantly stronger (da Rocha Dias et al., 2005; Grbovic et al., 2006). The S13A mutation in Cdc37 (Cdc37^{S13A}) is known to impact client interaction and maturation, likely at later stages of stable ternary complexes involving Hsp90, while its impact on the formation of the unstable binary complex is low. This allows complex recovery when the overexpression of both client and Cdc37 increases the population of binary complex intermediates (Liu and Landgraf, 2015). However, while the impairment in Cdc37 complex recovery is far more pronounced for the AEE mutant, the mutant still discriminates between wild-type and bRaf^{V600E}. The decrease in AEE mutant recovery is proportional to the difference seen for the interaction of wild-type Cdc37 with bRaf versus bRaf^{V600E}. Together with the comparable expression levels of wild-type and mutant Cdc37, this suggests that the ability to discern both forms of bRaf is retained and C-Cdc37 mutations do not achieve their disruptive impact through global destabilization and structure perturbation.

N-Cdc37 Is a Bona Fide Kinase Recognition Module

Despite the synergy between N- and C-Cdc37 in stabilizing binary Cdc37-client complexes, isolated C-Cdc37, or a two-domain construct comprised of M- and C-Cdc37 (MC-Cdc37) or NΔ30-Cdc37, does not interact with bRaf (Figure S5A). This is consistent with a model in which interaction of clients with C-Cdc37 is controlled by N-Cdc37 and suggests that Cdc37-kinase complexes are formed through a staged process where N-Cdc37 recognizes a client kinase and facilitates stable association with C-Cdc37. To test this hypothesis, we first investigated the interaction of N-Cdc37 with bRaf. In yeast, this is the minimal functional domain of the cochaperone (Lee et al., 2002; Turnbull et al., 2005), while in human cancer cells it is able to promote client association to Hsp90 (Smith et al., 2015). The

thermodynamic signature of binding is comparable to that of the full-length Cdc37, resulting, however, in a marginally higher affinity (0.09 μM versus 0.2 μM; Figures S5B and S5C), presumably due to the presence of an autoinhibitory element in the full-length Cdc37. Since NΔ30-Cdc37 is devoid of kinase binding, we also examined the interaction of bRaf with a peptide spanning the first 32 residues of Cdc37 (N32). Intriguingly, the thermodynamic signature of N32 binding to bRaf is distinct from that of N-Cdc37 or Cdc37 and is characterized by small favorable enthalpic and entropic contributions, which nevertheless result in one order magnitude lower affinity for the kinase (Figures S5B and S5C). Thus, although N32 encompasses the minimal kinase specificity determinants of Cdc37, it functions synergistically with other regions of N-Cdc37 to increase the affinity of the interaction by ~14-fold.

The low stability of bRaf in the presence of N-Cdc37 prevented us from revealing this complete set of kinase-binding determinants by NMR. However, the high specificity of Cdc37 for protein kinases (Taipale et al., 2012) suggests that N-Cdc37 comprises a general kinase-recognition domain, and we hypothesized that it recognizes clients and nonclients through a common mechanism. Thus, we followed the interaction of phosphorylated N-Cdc37 (pN-Cdc37) with a nonclient state of bRaf, represented by bRaf in complex with vemurafenib (*vem*-bRaf) (Polier et al., 2013; Taipale et al., 2012). We also used p38a as a protein kinase that does not exhibit Hsp90 dependency in its mature form (Taipale et al., 2012). Both kinases affect the ^{1}H-^{15}N HSQC of pN-Cdc37 in exactly the same way, producing small ($\Delta\delta_{max}$ ~0.04 ppm) and gradual CSPs, in a kinase-concentration-dependent manner (Figures 5A, 5B, and S5D). This result suggests that complex formation occurs at the fast exchange regime of the NMR timescale ($k_{ex} >> |\Delta\nu|$) and is reminiscent of a low-affinity, transient interaction. Nevertheless, the mode of nonclient kinase recognition by pN-Cdc37 is specific, as two unrelated kinases perturb the signals of the same subset of residues. These colocalize into two clusters, spanning the 40 N-terminal residues (W7, H9, pS13, D14, D15, T19, H20, N22, I23, D24, S27, L28, F29, W31, R39, and E41) and a smaller segment at the C-terminal end of the domain (M112 and W114). Comparison of signal intensities in the presence and absence of *vem*-bRaf reveals a similar differential effect. Kinase addition causes a uniform decrease in the intensity of all signals (~30%), but residues in the segments 1–44 and 110–116 exhibit significant signal attenuation with minima at W7, F29, and W114 (Figure 5C). Signal attenuation is a result of increased linewidth, as expected when a highly dynamic segment forms a complex with a 27 kDa protonated protein. When this set of residues is mapped on the structure of N-Cdc37, it is evident that the beginning of helix α_1 and the end of helix α_2 are regions of the two-helix bundle that are also involved in the interaction with kinases and thus may account for the significant increase in affinity when going from N32 to N-Cdc37 (Figures 5C and 5D). The role of the 42–109 region of the two-helix bundle is purely structural, that is, to bring the two kinase-interacting regions of N-Cdc37 in close proximity. The N-Cdc37-interacting segments identified for clients (Figure 2E) and nonclients (Figures 5D and S5E) are in excellent agreement, suggesting that recognition and specificity toward kinases occurs through a common mechanism for both classes. As for the interaction of the full-length protein with the client state of bRaf, S13 phosphorylation has no impact on the interaction

with nonclient kinases, and addition of p38 to nonphosphorylated N-Cdc37 results in identical CSPs and line broadening, as for the phosphorylated form (Figure 5B).

Combined with the information obtained for the Cdc37-bRaf interaction using methyl-TROSY, these data suggest that N-Cdc37 acts as a scanning factor of Cdc37 sampling for protein kinase catalytic domains through a mechanism that allows for the recognition of both Hsp90 clients and nonclients.

Cdc37 Selectively Alters the Conformational Properties of Client Kinases

Based on the differential mode of kinase recognition exhibited by Cdc37, where nonclients form transient complexes through only N-Cdc37, while clients form stable complexes through an interface that involves C-Cdc37, we hypothesized that Cdc37 does not function simply as a kinase specificity cochaperone, but it sorts kinases within the client-nonclient continuum. To test this hypothesis, we first examined the conformational properties of the two states of bRaf. Analysis of the fingerprint ^{1}H-^{15}N HSQC spectrum of bRaf is very informative about its structural and dynamic properties, even in the absence of assignment (Figure S6A). The observed signal dispersion and narrow linewidths suggest that prior to its interaction with the chaperone machinery, it represents a well-folded and monomeric kinase domain. However, the thermal stability of free bRaf is very low. Unfolding begins at 28°C and displays a sharp transition with a T_m of only 33.2°C (Figure S6B). It is noted that 205 signals out of the 265 expected appear in the spectrum, suggesting that despite being well folded, bRaf contains regions that undergo conformational exchange at a millisecond timescale. Exchange broadening is common in kinase NMR spectra and correlates to the intrinsic plasticity of regions that sample alternate conformations during kinase activation and catalysis, and particularly of the activation segment and hinge region. However, the large number of exchange-broadened signals observed indicates that bRaf contains extended dynamic regions that result in an overall low thermal stability. Comparison with the spectrum of *vem*-bRaf reveals chemical shift changes over the entire spectrum and the appearance of a large number of signals (251 in total) (Figure S6A). This marked effect indicates that ligand binding induces global changes in the structural and dynamic properties of bRaf, which is reflected in a large increase in T_m (~20°C) (Figure S6B). Thus, Cdc37 utilizes distinct modes of kinase recognition for the two bRaf states by sensing the enhanced conformational heterogeneity of the client over the nonclient state.

Since a common functional output of the Hsp90 chaperone cycle is to increase substrate stability, we hypothesized that Cdc37 binding to bRaf would quench its dynamic properties, especially if binding occurs at the regions that experience exchange broadening. However, comparison of the ^{1}H-^{13}C HMQC maps of free and Cdc37-bound bRaf reveals that upon addition of Cdc37 signals fall within any of the four classes: remain unaffected, broaden beyond detection, shift without a change in linewidth, or shift to the center of the spectrum with a very narrow linewidth (Figures 6A and S6C). This intriguing observation suggests that cochaperone binding enhances, rather than suppresses, the dynamics of the client kinase. Specifically, it induces local unfolding at some segments (as evident by the appearance of sharp signals at the “unfolded” region), while other segments form a heterogeneous ensemble of conformations that interconvert at a millisecond timescale (as

evident by the extreme broadening of other signals). Cdc37-induced unfolding is also observed for $bRaf^{V600E}$ (Figure S6C), which exhibits the same T_m as the wild-type kinase domain (Figure S6B) and, again, cannot interact with MC-Cdc37 in the absence of N-Cdc37 (Figure S6D).

In order to identify regions of the kinase domain that undergo unfolding transitions, we subjected bRaf, Cdc37, and Cdc37-bRaf to limited proteolysis using Lys-C and chymotrypsin. We then identified “conformotypic peptides” (Feng et al., 2014) using mass spectrometry. As expected based on our observations by NMR, in the presence of Cdc37 the proteolytic efficiency of both enzymes is markedly enhanced for some sites, while additional, unique cleavage sites are also identified (Figures S6E and S6F; Supplemental Information). Notably, enhanced proteolytic susceptibility, and thus conformational flexibility, is not limited in and around the ATP-binding cleft of the kinase domain but spans conserved features of the C-lobe and includes residues with limited solvent exposure (Figures 6B and 6C).

The functional role of the cochaperone-induced conformational destabilization becomes evident when the Hsp90-bRaf interaction is considered in the absence of Cdc37. Hsp90 addition to VLIMA-labeled bRaf causes only small shifts and broadening for a small group of signals in the ^{1}H-^{13}C HMQC spectrum (Figure S6G). This is consistent with a dynamic, transient interaction and is in agreement with previous observations showing that Hsp90 and bRaf do not coelute in the absence of Cdc37, despite the fact that stable Hsp90-Cdc37-bRaf complexes are formed (Polier et al., 2013). Notably, the set of methyl signals affected by Hsp90 belongs to the set of signals that either broaden or shift to the unfolded region upon Cdc37 addition. Thus, the Hsp90 binding sites on the catalytic core of a client kinase are only partly exposed, and stable association requires cochaperone-induced local unfolding.

In contrast to bRaf, the interaction of Cdc37 with *vem*-bRaf is dynamic and does not alter the conformational properties of the substrate. Addition of deuterated Cdc37 to VLIMA-labeled *vem*-bRaf has a negligible effect on either the linewidths or the positions of ^{1}H-^{13}C HMQC signals (Figure S6H), while the addition of unlabeled Cdc37 to ^{15}N-labeled *vem*-bRaf induces only minor chemical shift changes and broadening of few signals, which is consistent with a local and transient mode of interaction that is not accompanied by conformational change (Figure S6I).

In summary, although the specificity determinants of the substrate recognized by Cdc37 as a kinase fold are exposed in both the client and nonclient states of bRaf (Figures 2 and 5), the cochaperone senses the underlying differential dynamics and thermal stability of the two states by selectively altering the conformational manifold of only client kinase states. This altered conformational state, which encompasses partially unfolded regions from both kinase lobes, promotes interaction with the cochaperone through an interface that includes C-Cdc37, and presumably is poised for high affinity interaction with Hsp90.

N- and C-Cdc37 Have Compensatory Effects on Client's Conformational Stability

To further characterize the conformational properties of Cdc37-associated bRaf, we monitored changes in the fluorescence spectrum of 1-anilinonaphthalene-8-sulfonic acid

(ANS). Cdc37 or N-Cdc37 produces only small changes to the spectrum of ANS (Figure 6D), indicating that all three domains possess a compact tertiary structure without exposed hydrophobic cavities. However, bRaf does alter the spectroscopic properties of ANS, producing a large increase in intensity and a blue shift of the emission maximum. This result indicates that the client state of bRaf contains accessible hydrophobic pockets that bind ANS (Betzi et al., 2011) and possibly inherently unstable regions (Figure 6D). However, in the presence of the binary Cdc37-bRaf complex, the emission intensity of ANS is significantly higher than it is in the presence of either of the two free proteins or the sum of their emission spectra (Figure S7A). Notably, the effect becomes more pronounced in the presence of the N-Cdc37-bRaf binary complex, producing higher emission intensity and a significant blue shift. On the other hand, the increase in emission intensity is very small for the Cdc37-*vem*-bRaf mixture and is comparable to the sum of intensities of the free proteins, indicating that the nonclient state does not undergo local unfolding (Figure S7B).

These data suggest that N-Cdc37 comprises the region of the cochaperone that induces a metastable conformation to the kinase, which is partly stabilized by the interface presented by C-Cdc37 when the full-length protein is considered.

DISCUSSION

The sequential interaction of cochaperones with Hsp90 fine-tunes the progression of the chaperone cycle (Röhl et al., 2013). Here we demonstrate that the function of Cdc37 as a substrate recruiter cochaperone is not strictly that of an adaptor protein, but instead is to actively participate in making triage decisions as to which substrates require stable association with Hsp90 (Figure 7). The functionally indispensable N-Cdc37 has a dual role: first, it acts as a kinase-scanning factor with broad kinase specificity, and second, it exhibits client-sorting activity by selectively locally unfolding only client kinases. This transition triggers stable client association through a cochaperone interface provided by C-Cdc37. Thus, Cdc37 performs a quality control of protein kinases, where a cochaperone-induced metastable conformational state acts as a “flag” for stable cochaperone association and thus Hsp90 dependence.

Specificity of Cdc37 to Protein Kinases

N-Cdc37 plays critical roles in kinase recognition (Eckl et al., 2015; Polier et al., 2013; Shao et al., 2003a; Vaughan et al., 2006; Xu et al., 2012) and regulation of Hsp90's conformational switching (Shao et al., 2003b). We show that it forms an independently folded helical domain that contains long dynamic segments at the N- and C-terminal ends (Figure 1). A peptide that spans the first 32 residues recognizes client kinases but exhibits moderate affinity as compared to N-Cdc37 or Cdc37 (Figure S5). The conformational plasticity of N32 is expected to be important for the recognition of the conserved, but nevertheless diverse, group of client kinases. Using model client and nonclient kinases, we reveal that the complete kinase recognition elements within N-Cdc37 reach beyond the flexible N terminus and include short segments at the beginning of helix α_1 and the end of helix α_2 (Figures 2E and 5). Although N-Cdc37 recognizes client and nonclient kinases through the same set of elements, client kinases are engaged in stable Cdc37 complexes

through additional contacts provided by a newly identified conserved hydrophobic surface on C-Cdc37. Access to the C-Cdc37 binding site is, however, under the control of N-Cdc37, as constructs that lack N32 are devoid of kinase binding. Compromising the overall hydrophobicity of C-Cdc37's site impacts the chaperone function of Cdc37 (Figure 4). This is consistent with previous studies performed with *Drosophila* Cdc37, where the W342C mutation, which contributes to the overall hydrophobicity of the binding site, had a detrimental effect on kinase-mediated signaling (Cutforth and Rubin, 1994). In contrast, Y298 is not located in this surface, and thus, the regulatory role of this phosphorylation switch is probably indirect. The hydroxyl group of Y298 is in the vicinity of D310 (Zhang et al., 2015), and phosphorylation would result in structural destabilization by electrostatic repulsion. In addition, C-Cdc37 is expected to face away from the main body of an Hsp90-Cdc37-kinase complex (Vaughan et al., 2006), and M-Cdc37 binding to N-Hsp90 (N-terminal domain of Hsp90) may trigger transfer of the substrate from C-Cdc37 to Hsp90. Indeed, our data suggest that the state of bRaf binding to N- and C-Cdc37 is transmitted to M-Cdc37.

Cdc37-Mediated Sorting Activity

Protein kinases do not fall into a binary client-nonclient classification, but rather are sorted within a continuum that spans the two extremes. Recent findings suggest that the Hsp90 machinery sorts substrates by “sensing” their thermal stability (Boczek et al., 2015; Taipale et al., 2012, 2013), and thermally unstable kinase domains exhibit strong Hsp90 dependence, while thermally stable kinase domains show only weak functional dependence. The apparent correlation between Cdc37 and Hsp90 association suggests that Cdc37 may play a direct role in this process. Our in vitro studies using bRaf show that Cdc37 comprises the subunit of the Hsp90 machinery that “senses” kinase stability and implicate the cochaperone directly in the process of kinase sorting. The soluble bRaf variant we used as a model represents a mature form of a kinase domain that has been processed by early bacterial chaperone complexes (Chapman et al., 2006) (Calloni et al., 2012). Although it populates a near-native conformation, it contains conformationally labile regions that result in a marginal thermal stability (Figures 6 and S6). Cdc37 acts as a stability sensor by altering its conformational landscape and shifting the population from the native state toward an ensemble of nonnative conformations (Figures 6 and S6). An extended interface presented by C-Cdc37 holds the metastable client and thus prevents nonnative intermolecular contacts and aggregation. On the other hand, Cdc37 is not effective in modifying the conformational landscape of the nonclient state of bRaf. Despite the fact that this state is recognized as a kinase domain by N-Cdc37, its significantly higher thermal stability makes it insensitive to the destabilizing effect of the cochaperone. Thus, Cdc37 subjects kinase catalytic domains to a controlled conformational stress as a mechanism of sorting client kinases.

Consequences for Hsp90 Kinase Loading

Two cryoelectron microscopy (cryo-EM) structures (Vaughan et al., 2006; Verba et al., 2016) have shown that kinase domains interact with Hsp90 in an extended conformation, indicating that they undergo a large-scale structural rearrangement when in complex with Hsp90. However, Hsp90 does not form stable complexes with either bRaf or Cdk4 (Polier et al., 2013; Vaughan et al., 2006), despite the fact that the corresponding stable ternary Hsp90-

Cdc37-kinase complexes can be formed. This is consistent with our NMR data showing that in contrast to Cdc37, Hsp90 interacts with bRaf in a dynamic fashion, without altering its conformational properties (Figure S6G). Hence, beyond its role as an adaptor protein, Cdc37 can be involved in lowering the acti vation barrier for the structural rearrangement of the kinase that leads to stable association with Hsp90. Indeed, most protein kinases exhibit similar dissociation rates from Hsp90 upon inhibition, implying that kinase-binding on rates determine the level of association with the chaperone (Taipale et al., 2012). The conformationally labile state of Cdc37-bound bRaf may represent a preselected open structure of the kinase, where the two lobes are separated and thus are presented to Hsp90 with an optimal relative orientation. Alternatively, the regions of bRaf that sample nonnative conformations in the presence of Cdc37 may enhance the interaction with Hsp90, which subsequently performs the structural reorganization of the substrate. Although these models are not mutually exclusive, our observation that the regions of the native kinase state recognized by Hsp90 are in part common to those sampling nonnative conformations when bound to Cdc37 (Figure S6G) suggest that local unfolding may simply increase the affinity of these sites for Hsp90. It is plausible to assume that stable association of Cdk4 with Hsp90 occurs through a similar Cdc37-mediated conformational rearrangement of the kinase domain that involves partial unfolding. In this respect, the latest high-resolution cryo-EM structure of Hsp90-Cdc37-Cdk4 shows that the β_4-β_5 strands and αC-β_4 loop of Cdk4 are completely unfolded, allowing the two kinase lobes to become separated (Verba et al., 2016). Notably, these structural elements partially overlap with the bRaf regions that expose unique proteolytic sites in complex with Cdc37 (Figures 4B and 4C; Supplemental Information) and, particularly, the αC-β4 loop and the beginning of β_4 strand. The proposed model of local unfolding for efficient kinase transfer to Hsp90 is also consistent to the mode of steroid hormone receptor transfer to Hsp90 (Kirschke et al., 2014). In this case, the Hsp70/Hsp40 system partially unfolds the ligand binding domain of the receptor in the vicinity of the ligand binding site, prior to transfer to Hsp90.

Finally, our findings reconcile previous observations regarding kinase transfer to Hsp90 when a direct Cdc37-Hsp90 interaction is restricted (Smith et al., 2015). We show that N-Cdc37 acts as an allosteric effector on the kinase by altering its conformational properties and providing an indirect route for a productive association with Hsp90- (Lee et al., 2002; Scholz et al., 2000; Smith et al., 2015; Turnbull et al., 2005) or C-Cdc37-containing constructs (Eckl et al., 2015).

EXPERIMENTAL PROCEDURES

Sample Preparations and Isotope Labeling

Cdc37, N-Cdc37, MC-Cdc37, and C-Cdc37 constructs were expressed and purified as described previously (Zhang et al., 2015). Labeled or unlabeled bRaf, NM-Cdc37, p38, and Hsp90$\alpha\beta$1 were obtained as described in the Supplemental Information. Point mutants were generated using the QuikChange II XL Site-Directed Mutagenesis Kit (Agilent). Cdc37 and N-Cdc37 phosphorylation at position S13 was performed using CKII holoenzyme (NEB) as described in the Supplemental Information. A peptide corresponding to the 32 aminoterminal residues of human Cdc37 was obtained synthetically with His33 substituted

for a Cys. All experiments were carried out in 20 mM Tris (pH 7.5), 100 mM NaCl, 0.5 mM EDTA, and 2.5 mM DTT, unless otherwise stated in the Supplemental Information.

NMR Spectroscopy and N-Cdc37 Model

NMR experiments were performed on Varian direct drive 600 and 800 MHz spectrometers equipped with a cryoprobe. Assignment of backbone atoms for N-Cdc37 was obtained by standard triple-resonance pulse sequences, aided by selective amino acid labeling/unlabeling and a 3D HNN experiment (Panchal et al., 2001). Sidechain and methyl group assignment was accomplished with TOCSY-based experiments, in combination with side-directed mutagenesis. Methyl group assignment transfer from isolated domains to full-length Cdc37 was assisted by a 3D HMQC-NOESY-HMQC spectrum acquired in D_2O and further aided by a series of mutants at linker regions. All spectra were processed with NMRpipe (Delaglio et al., 1995) and analyzed using sparky (T.D. Goddard and D.G. Kneller, SPARKY 3, University of California, San Francisco). NOE restraints were derived from a 3D ^{15}N-edited NOESY-HSQC and a 3D HMQC-NOESY-HMQC. Pairs of unambiguously assigned NOEs, TALOS-derived dihedral angles (Shen and Bax, 2013), and a set of hydrogen bonds were incorporated as restraints in CYANA 2.1 (Güntert et al., 1997).

Supplementary Material

Refer to Web version on PubMed Central for supplementary material.

ACKNOWLEDGMENTS

We are grateful to Dr. E. Schönbrunn (H. Lee Moffitt Cancer Center) for providing us with the plasmid for Hsp90αβ1, Dr. G. Daughdrill for access to a VP-ITC, Dr. Tara Word for assistance with fluorescence measurements, Dr. D. Chaput for assistance with mass spectrometry, and S. Feola and S. Kouvaras for assistance with sample preparations. NMR and mass spectrometry were carried out at USF's Florida Center of Excellence for Drug Discovery and Innovation. This work was supported in part by the American Cancer Society (IRG93-032-16 to I.G.) and the NIH (GM115854 to I.G.).

REFERENCES

Betzi S, Alam R, Martin M, Lubbers DJ, Han H, Jakkaraj SR, Georg GI, Schönbrunn E. Discovery of a potential allosteric ligand binding site in CDK2. ACS Chem. Biol. 2011; 6:492–501. [PubMed: 21291269]

Boczek EE, Reefschläger LG, Dehling M, Struller TJ, Häusler E, Seidl A, Kaila VR, Buchner J. Conformational processing of oncogenic v-Src kinase by the molecular chaperone Hsp90. Proc. Natl. Acad. Sci. USA. 2015; 112:E3189–E3198. [PubMed: 26056257]

Calloni G, Chen T, Schermann SM, Chang HC, Genevaux P, Agostini F, Tartaglia GG, Hayer-Hartl M, Hartl FU. DnaK functions as a central hub in the E. coli chaperone network. Cell Rep. 2012; 1:251–264. [PubMed: 22832197]

Caplan AJ, Mandal AK, Theodoraki MA. Molecular chaperones and protein kinase quality control. Trends Cell Biol. 2007; 17:87–92. [PubMed: 17184992]

Chapman E, Farr GW, Usaite R, Furtak K, Fenton WA, Chaudhuri TK, Hondorp ER, Matthews RG, Wolf SG, Yates JR, et al. Global aggregation of newly translated proteins in an Escherichia coli strain deficient of the chaperonin GroEL. Proc. Natl. Acad. Sci. USA. 2006; 103:15800–15805. [PubMed: 17043235]

Citri A, Harari D, Shohat G, Ramakrishnan P, Gan J, Lavi S, Eisenstein M, Kimchi A, Wallach D, Pietrokovski S, Yarden Y. Hsp90 recognizes a common surface on client kinases. J. Biol. Chem. 2006; 281:14361–14369. [PubMed: 16551624]

Cutforth T, Rubin GM. Mutations in Hsp83 and cdc37 impair signaling by the sevenless receptor tyrosine kinase in Drosophila. Cell. 1994; 77:1027–1036. [PubMed: 8020093]

da Rocha Dias S, Friedlos F, Light Y, Springer C, Workman P, Marais R. Activated B-RAF is an Hsp90 client protein that is targeted by the anticancer drug 17-allylamino-17-demethoxygeldanamycin. Cancer Res. 2005; 65:10686–10691. [PubMed: 16322212]

Delaglio F, Grzesiek S, Vuister GW, Zhu G, Pfeifer J, Bax A. NMRPipe: a multidimensional spectral processing system based on UNIX pipes. J. Biomol. NMR. 1995; 6:277–293. [PubMed: 8520220]

Eckl JM, Scherr MJ, Freiburger L, Daake MA, Sattler M, Richter K. Hsp90-Cdc37 complexes with protein kinases form cooperatively with multiple distinct interaction sites. J. Biol. Chem. 2015; 290:30843–30854. [PubMed: 26511315]

Feng Y, De Franceschi G, Kahraman A, Soste M, Melnik A, Boersema PJ, de Laureto PP, Nikolaev Y, Oliveira AP, Picotti P. Global analysis of protein structural changes in complex proteomes. Nat. Biotechnol. 2014; 32:1036–1044. [PubMed: 25218519]

Fraczkiewicz R, Braun W. Exact and efficient analytical calculation of the accessible surface areas and their gradients for macromolecules. J. Comput. Chem. 1998; 19:319–333.

Grbovic OM, Basso AD, Sawai A, Ye Q, Friedlander P, Solit D, Rosen N. V600E B-Raf requires the Hsp90 chaperone for stability and is degraded in response to Hsp90 inhibitors. Proc. Natl. Acad. Sci. USA. 2006; 103:57–62. [PubMed: 16371460]

Güntert P, Mumenthaler C, Wüthrich K. Torsion angle dynamics for NMR structure calculation with the new program DYANA. J. Mol. Biol. 1997; 273:283–298. [PubMed: 9367762]

Karnitz LM, Felts SJ. Cdc37 regulation of the kinome: when to hold ‘em and when to fold ’em. Sci. STKE. 2007; 2007:pe22. [PubMed: 17488976]

Kirschke E, Goswami D, Southworth D, Griffin PR, Agard DA. Glucocorticoid receptor function regulated by coordinated action of the Hsp90 and Hsp70 chaperone cycles. Cell. 2014; 157:1685–1697. [PubMed: 24949977]

Lee P, Rao J, Fliss A, Yang E, Garrett S, Caplan AJ. The Cdc37 protein kinase-binding domain is sufficient for protein kinase activity and cell viability. J. Cell Biol. 2002; 159:1051–1059. [PubMed: 12499358]

Liu W, Landgraf R. Phosphorylated and unphosphorylated serine 13 of CDC37 stabilize distinct interactions between its client and HSP90 binding domains. Biochemistry. 2015; 54:1493–1504. [PubMed: 25619116]

Miyata Y, Nishida E. CK2 controls multiple protein kinases by phosphorylating a kinase-targeting molecular chaperone, Cdc37. Mol. Cell. Biol. 2004; 24:4065–4074. [PubMed: 15082798]

Panchal SC, Bhavesh NS, Hosur RV. Improved 3D triple resonance experiments, HNN and HN(C)N, for HN and 15N sequential correlations in (13C, 15N) labeled proteins: application to unfolded proteins. J. Biomol. NMR. 2001; 20:135–147. [PubMed: 11495245]

Polier S, Samant RS, Clarke PA, Workman P, Prodromou C, Pearl LH. ATP-competitive inhibitors block protein kinase recruitment to the Hsp90-Cdc37 system. Nat. Chem. Biol. 2013; 9:307–312. [PubMed: 23502424]

Prince T, Matts RL. Definition of protein kinase sequence motifs that trigger high affinity binding of Hsp90 and Cdc37. J. Biol. Chem. 2004; 279:39975–39981. [PubMed: 15258137]

Roe SM, Ali MM, Meyer P, Vaughan CK, Panaretou B, Piper PW, Prodromou C, Pearl LH. The mechanism of Hsp90 regulation by the protein kinase-specific cochaperone p50(cdc37). Cell. 2004; 116:87–98. [PubMed: 14718169]

Röhl A, Rohrberg J, Buchner J. The chaperone Hsp90: changing partners for demanding clients. Trends Biochem. Sci. 2013; 38:253–262. [PubMed: 23507089]

Scholz G, Hartson SD, Cartledge K, Hall N, Shao J, Dunn AR, Matts RL. p50(Cdc37) can buffer the temperature-sensitive properties of a mutant of Hck. Mol. Cell. Biol. 2000; 20:6984–6995. [PubMed: 10958693]

Scroggins BT, Prince T, Shao J, Uma S, Huang W, Guo Y, Yun BG, Hedman K, Matts RL, Hartson SD. High affinity binding of Hsp90 is triggered by multiple discrete segments of its kinase clients. Biochemistry. 2003; 42:12550–12561. [PubMed: 14580201]

Shao J, Irwin A, Hartson SD, Matts RL. Functional dissection of cdc37: characterization of domain structure and amino acid residues critical for protein kinase binding. Biochemistry. 2003a; 42:12577–12588. [PubMed: 14580204]

Shao J, Prince T, Hartson SD, Matts RL. Phosphorylation of serine 13 is required for the proper function of the Hsp90 co-chaperone, Cdc37. J. Biol. Chem. 2003b; 278:38117–38120. [PubMed: 12930845]

Shen Y, Bax A. Protein backbone and sidechain torsion angles predicted from NMR chemical shifts using artificial neural networks. J. Biomol. NMR. 2013; 56:227–241. [PubMed: 23728592]

Smith JR, de Billy E, Hobbs S, Powers M, Prodromou C, Pearl L, Clarke PA, Workman P. Restricting direct interaction of CDC37 with HSP90 does not compromise chaperoning of client proteins. Oncogene. 2015; 34:15–26. [PubMed: 24292678]

Sreeramulu S, Gande SL, Göbel M, Schwalbe H. Molecular mechanism of inhibition of the human protein complex Hsp90-Cdc37, a kinome chaperone-cochaperone, by triterpene celastrol. Angew. Chem. Int. Ed. Engl. 2009a; 48:5853–5855. [PubMed: 19585625]

Sreeramulu S, Jonker HR, Langer T, Richter C, Lancaster CR, Schwalbe H. The human Cdc37.Hsp90 complex studied by hetero-nuclear NMR spectroscopy. J. Biol. Chem. 2009b; 284:3885–3896. [PubMed: 19073599]

Taipale M, Jarosz DF, Lindquist S. HSP90 at the hub of protein homeostasis: emerging mechanistic insights. Nat. Rev. Mol. Cell Biol. 2010; 11:515–528. [PubMed: 20531426]

Taipale M, Krykbaeva I, Koeva M, Kayatekin C, Westover KD, Karras GI, Lindquist S. Quantitative analysis of HSP90-client interactions reveals principles of substrate recognition. Cell. 2012; 150:987–1001. [PubMed: 22939624]

Taipale M, Krykbaeva I, Whitesell L, Santagata S, Zhang J, Liu Q, Gray NS, Lindquist S. Chaperones as thermodynamic sensors of drug-target interactions reveal kinase inhibitor specificities in living cells. Nat. Biotechnol. 2013; 31:630–637. [PubMed: 23811600]

Terasawa K, Minami Y. A client-binding site of Cdc37. FEBS J. 2005; 272:4684–4690. [PubMed: 16156789]

Thevakumaran N, Lavoie H, Critton DA, Tebben A, Marinier A, Sicheri F, Therrien M. Crystal structure of a BRAF kinase domain monomer explains basis for allosteric regulation. Nat. Struct. Mol. Biol. 2015; 22:37–43. [PubMed: 25437913]

Tsai J, Lee JT, Wang W, Zhang J, Cho H, Mamo S, Bremer R, Gillette S, Kong J, Haass NK, et al. Discovery of a selective inhibitor of oncogenic B-Raf kinase with potent antimelanoma activity. Proc. Natl. Acad. Sci. USA. 2008; 105:3041–3046. [PubMed: 18287029]

Turnbull EL, Martin IV, Fantes PA. Cdc37 maintains cellular viability in Schizosaccharomyces pombe independently of interactions with heat-shock protein 90. FEBS J. 2005; 272:4129–4140. [PubMed: 16098195]

Vaughan CK, Gohlke U, Sobott F, Good VM, Ali MM, Prodromou C, Robinson CV, Saibil HR, Pearl LH. Structure of an Hsp90-Cdc37-Cdk4 complex. Mol. Cell. 2006; 23:697–707. [PubMed: 16949366]

Vaughan CK, Mollapour M, Smith JR, Truman A, Hu B, Good VM, Panaretou B, Neckers L, Clarke PA, Workman P, et al. Hsp90-dependent activation of protein kinases is regulated by chaperone-targeted dephosphorylation of Cdc37. Mol. Cell. 2008; 31:886–895. [PubMed: 18922470]

Verba, KA.; Wang, RY.; Arakawa, A.; Liu, Y.; Shirouzu, M.; Yokoyama, S.; Agard, DA. Atomic structure of Hsp90:Cdc37:Cdk4 reveals Hsp90 regulates kinase via dramatic unfolding.. bioRxiv. 2016. Published online March 4, 2016. http://dx.doi.org/10.1101/040907

Xu Y, Lindquist S. Heat-shock protein hsp90 governs the activity of pp60v-src kinase. Proc. Natl. Acad. Sci. USA. 1993; 90:7074–7078. [PubMed: 7688470]

Xu Y, Singer MA, Lindquist S. Maturation of the tyrosine kinase c-src as a kinase and as a substrate depends on the molecular chaperone Hsp90. Proc. Natl. Acad. Sci. USA. 1999; 96:109–114. [PubMed: 9874780]

Xu W, Yuan X, Xiang Z, Mimnaugh E, Marcu M, Neckers L. Surface charge and hydrophobicity determine ErbB2 binding to the Hsp90 chaperone complex. Nat. Struct. Mol. Biol. 2005; 12:120–126. [PubMed: 15643424]

Xu W, Mollapour M, Prodromou C, Wang S, Scroggins BT, Palchick Z, Beebe K, Siderius M, Lee MJ, Couvillon A, et al. Dynamic tyrosine phosphorylation modulates cycling of the HSP90-P50(CDC37)-AHA1 chaperone machine. Mol. Cell. 2012; 47:434–443. [PubMed: 22727666]

Zhang Z, Keramisanou D, Dudhat A, Paré M, Gelis I. The C-terminal domain of human Cdc37 studied by solution NMR. J. Biomol. NMR. 2015; 63:315–321. [PubMed: 26400850]

Zhao Q, Boschelli F, Caplan AJ, Arndt KT. Identification of a conserved sequence motif that promotes Cdc37 and cyclin D1 binding to Cdk4. J. Biol. Chem. 2004; 279:12560–12564. [PubMed: 14701845]

Highlights

- Differential recognition of client and nonclient kinases
- Selective client association with C-Cdc37
- Cdc37 as a sensor of kinase thermal stability
- Induced kinase unfolding as a mechanism of client sorting

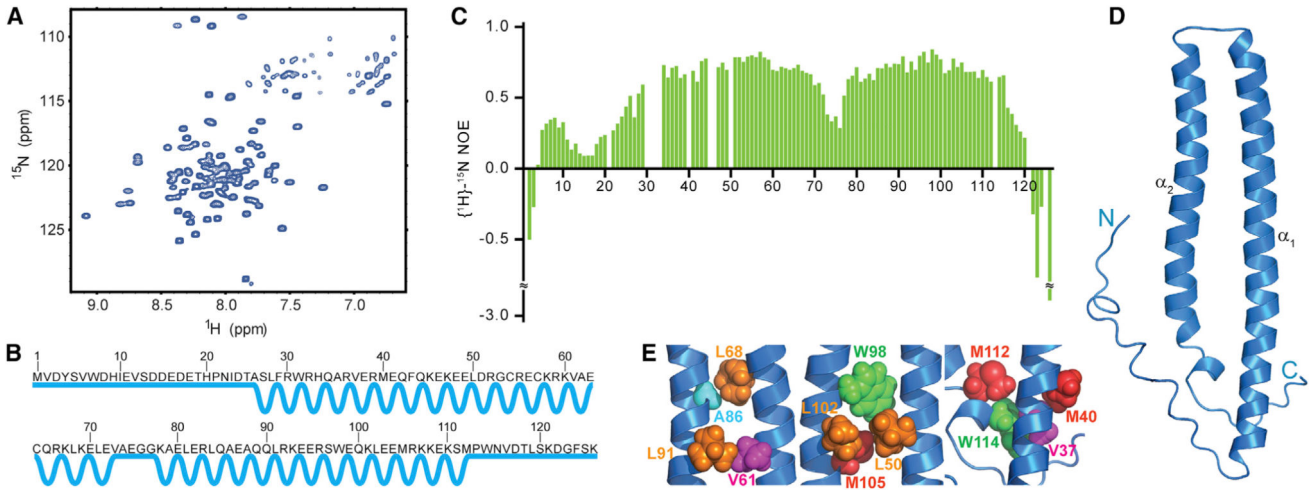

Figure 1. Structural and Dynamic Properties of N-Cdc37 in Solution

(A) The ^{1}H-^{15}N-HSQC spectrum of N-Cdc37 exhibits limited signal dispersion (the Trp indole region is omitted).

(B) N-Cdc37 secondary structure: straight and zigzag lines illustrate unstructured and helical regions, respectively.

(C) hNOE values as function of primary sequence. Missing values are due to prolines, missing assignment, or extreme overlap that precludes accurate quantitation.

(D) Ribbon diagram of the lowest energy structure of N-Cdc37 showing helices α_1 and α_2 and the terminal tails.

(E) Clusters of stabilizing nonpolar interactions between α_1 and α_2 identified by NMR and utilized for building a structural model (see also Figure S1).

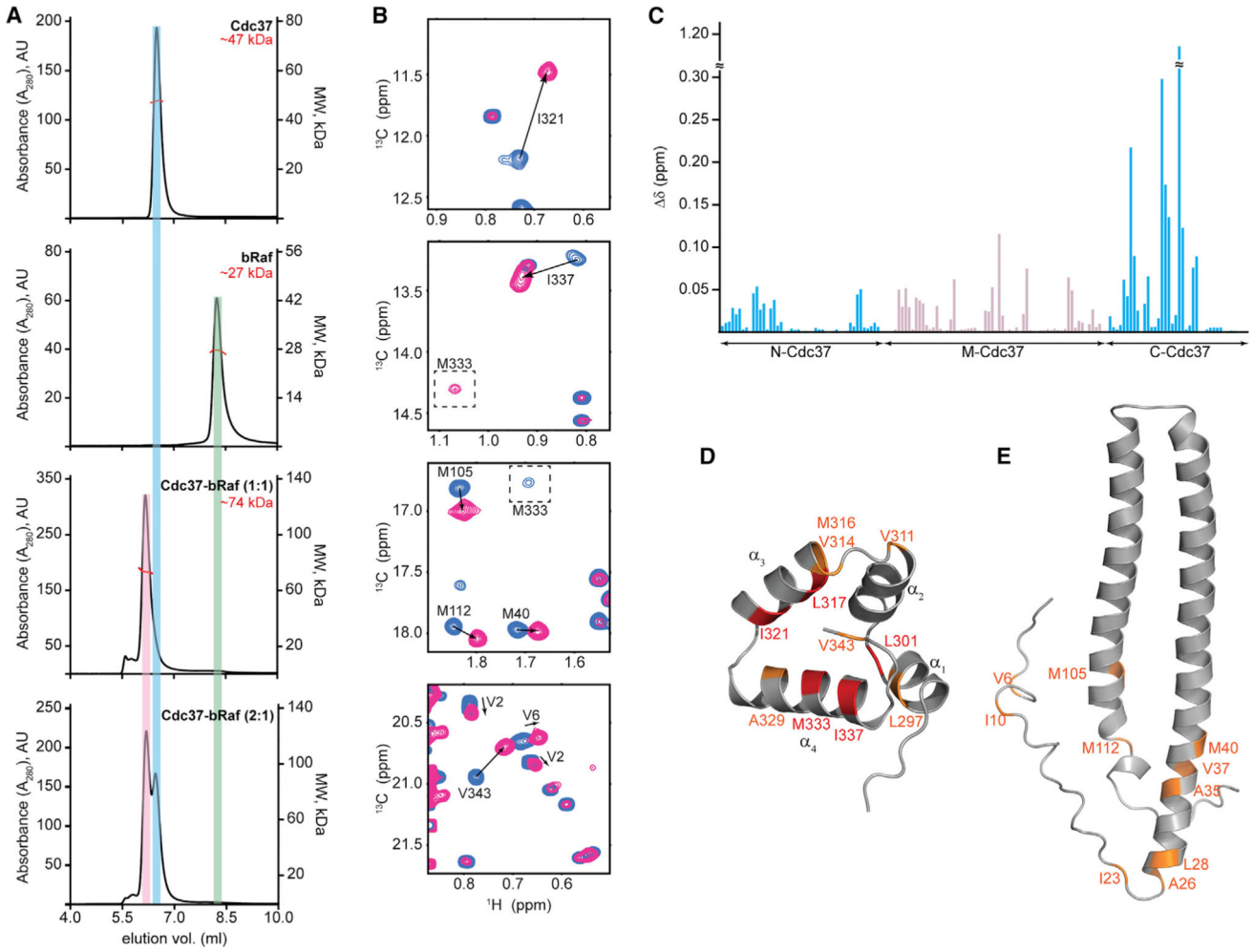

Figure 2. Assembly of Binary Cdc37-bRaf Complexes

(A) SEC-MALS traces, displayed from top to bottom for Cdc37 (49 μM), bRaf (34 μM), Cdc37 + bRaf (both at 80 μM), and Cdc37 + bRaf (at 80 μM and 40 μM, respectively).

(B) Selected regions of ^{1}H-^{13}C HMQC correlation maps of labeled Cdc37 in the absence (blue) or presence of 1.2 equivalents of unlabeled bRaf (pink). The signal for M333 shows the largest CSP and shifts near the “Ile” region.

(C) Magnitude of CSPs (Δδ) as a function of Cdc37 primary sequence. CSPs for methyl groups of N- and C-Cdc37 (aa 1–126 and 287–378, respectively) are shown in cyan. CSPs for M-Cdc37 methyl groups are displayed for those signals that split in the bound state (gray).

(D and E) Ribbon representation of C-Cdc37 (shown in D) and N-Cd37 (shown in E), highlighting residues that experience Δδ > 0.13 ppm (red) and 0.028 > Δδ > 0.13 ppm (orange) (see also Figures S2 and S3).

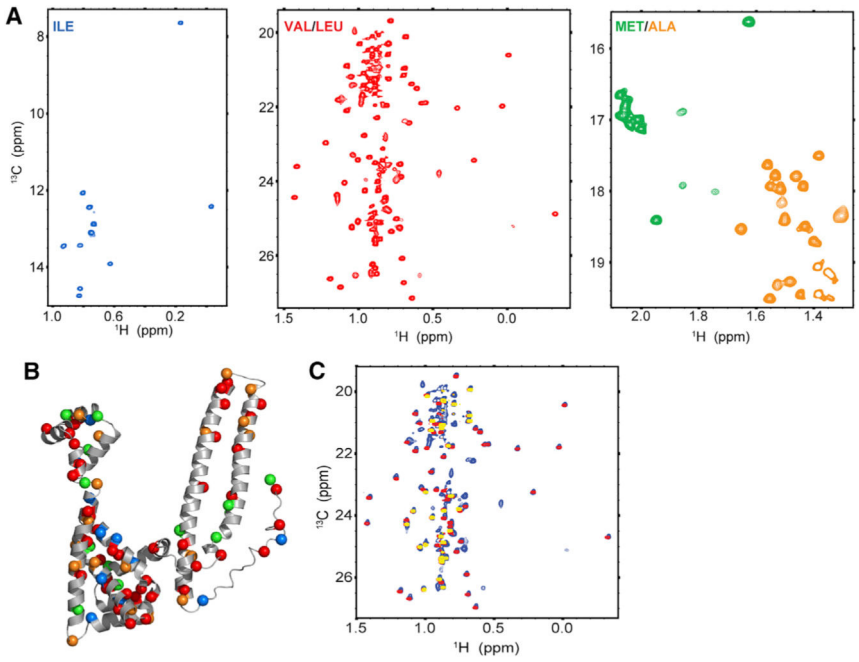

Figure 3. Methyl-TROSY NMR of Cdc37

(A) ^{1}H-^{13}C HMQC spectra of Cdc37 U-[^{2}H,^{12}C]-Ile$^{\delta 1}$-[$^{13}CH_3$] (blue), U-[^{2}H,^{12}C]-Val/Leu-[$^{13}CH_3$] (red), and U-[^{2}H,^{12}C]-Met-Ala-[$^{13}CH_3$] (green-orange).

(B) The Cα atoms of Cdc37 methyl-bearing amino acids used as probes to monitor interactions with bRaf are displayed as spheres on a pseudomodel of full-length Cdc37. The C terminus of the protein (342–378) is omitted. The color code is the same as in (A).

(C) Overlay of ^{1}H-^{13}C HMQC spectra, from the two-domain fragment comprised of N- and M-Cdc37 (1–276, red) and N-Cdc37 (yellow) onto the spectrum of full-length Cdc37 (blue).

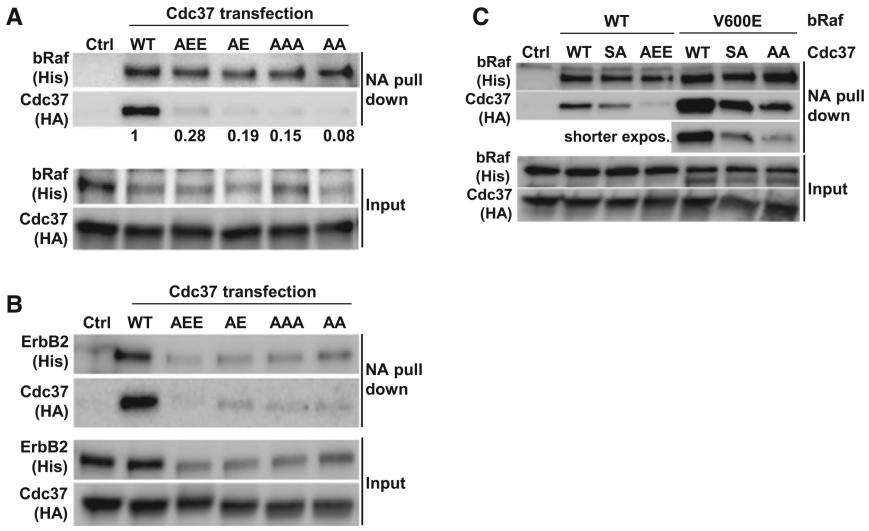

Figure 4. Mutations at C-Cdc37 Compromise the Formation of Binary Cdc37-Client Complexes in MCF7 When His-Tagged Cdc37 Is Transiently Coexpressed with Biotin-Tagged bRaf Client and BirA

(A) C-Cdc37 mutants show an all but complete loss of recovery in a pull-down analysis of bRaf with neutravidin beads. bRaf and Cdc37 were detected by their His and HA tags, as indicated. The control in all panels is equivalent to wild-type (WT) but uses biotin-saturated neutravidin beads. The relative efficiency of BirA-mediated biotinylation of bRaf is impaired for cotransfections with mutant Cdc37, and the ratio of biotinylated bRaf to recovered Cdc37 is shown for each mutant.

(B) All C-Cdc37 mutants reduce ErbB2-Cdc37 interactions. Compared to bRaf, synthesis of the slow maturing ErbB2 receptor is more impaired for all Cdc37 mutants while biotinylation efficiencies are more uniform.

(C) While $bRaf^{V600E}$ shows a substantially elevated Cdc37 association, the relative sensitivity of this complex to the AEE mutation is comparable to wild-type bRaf. The $bRaf^{V600E}$ recovery is shown at lower exposure setting to facilitate comparison of relative changes with wild-type bRaf. Consistent with the thermodynamic signature of $Cdc37^{S13A}$-bRaf binding (Figure S5B), the mutant has a reduced impact on an initial Cdc37-client binary complex, and it was added as a reference point (see also Figure S4).

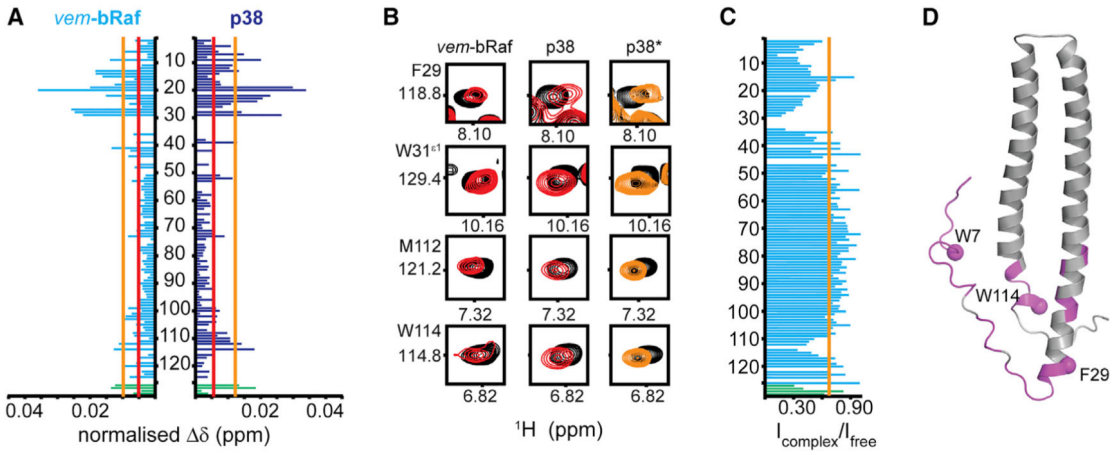

Figure 5. Interaction of N-Cdc37 with Nonclient Kinases

(A) CSP pattern for the interaction of pN-Cdc37 with *vem*-bRaf and p38. CSPs greater than the mean or one SD above the mean are marked by red and yellow lines, respectively.

(B) Representative set of HSQC signals affected by *vem*-bRaf or p38. The right panel (marked p38*) illustrates the same signals for the titration of N-Cdc37 with p38.

(C) Signal intensity ratio for free over *vem*-bRaf-bound pN-Cdc37. The average drop in intensity is marked by a yellow line.

(D) Residues for which significant signal attenuation is observed upon addition of *vem*-bRaf are highlighted on the structure of N-Cdc37. The Cα atoms of W7, F29, and W114, which experience the most prominent attenuation, are shown as spheres. In (A) and (C), signals of Trp ^{1}H-$^{15}N^{\varepsilon 1}$ pairs are shown in green bars (W7, W31, W85, and W114, top to bottom) (see also Figure S5).

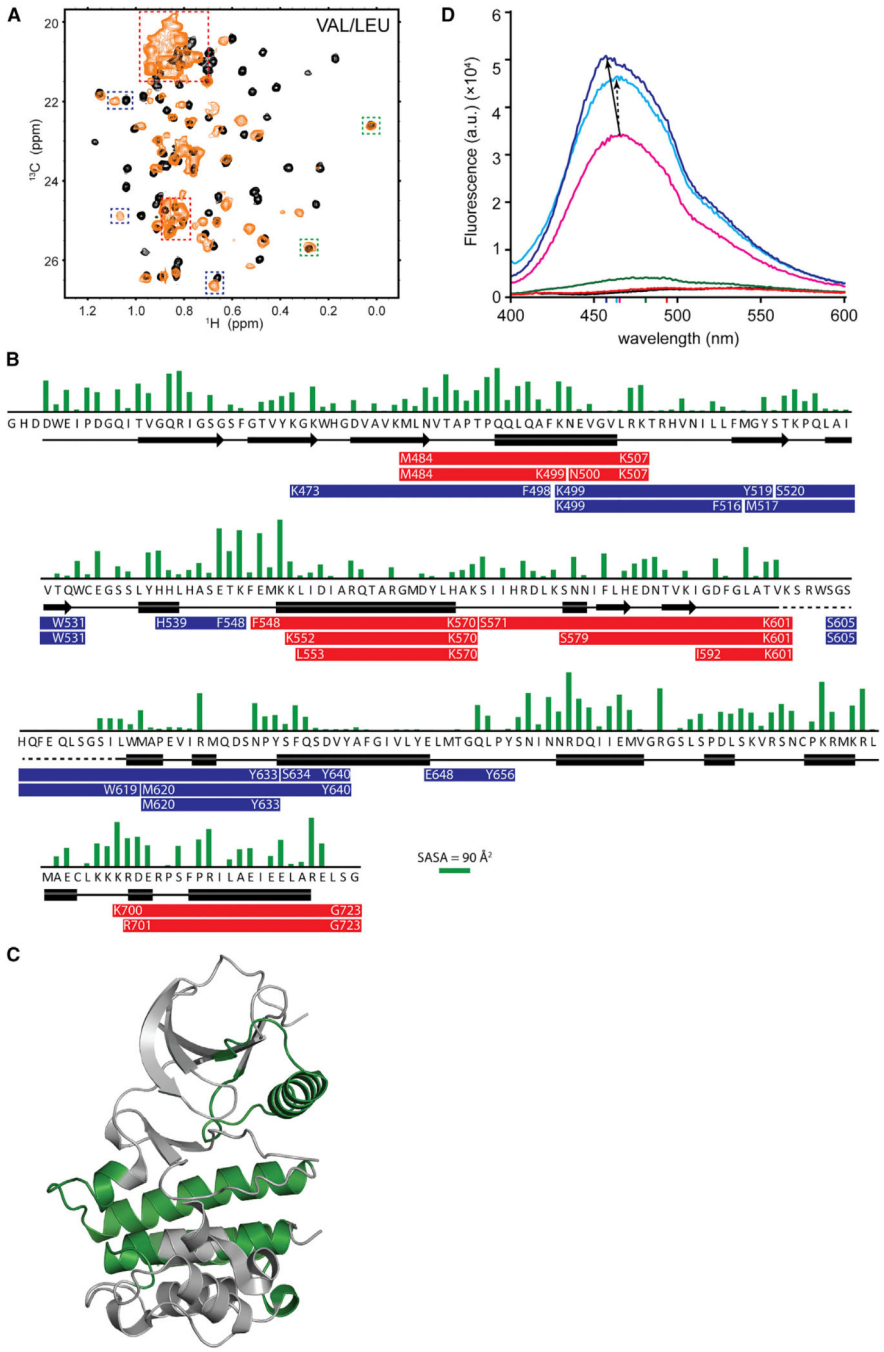

Figure 6. Cdc37 Alters the Conformational Properties of Client Kinases

(A) The ^{1}H-^{13}C HMQC spectrum of Val/Leu-labeled bRaf in the absence (black) or presence of 1.2 equivalents [U-^{2}H]-pCdc37 (yellow). Signals that shift to the unfolded region with narrow linewidths (red), show a shift (blue), or do not shift (green) are highlighted. For methyl groups showing a change in chemical shift, the signal for the free state disappears completely, in agreement with a 1:1 stoichiometry.

(B) Sidechain-solvent-accessible surface area (Fraczkiewicz and Braun, 1998) (green bars) and secondary structure (black symbols, PDB: 30G7) of solubilized bRaf as a function of

primary sequence. Proteolytic fragments uniquely identified in Cdc37-bound bRaf, or fragments that show enhanced abundance in the presence of Cdc37, after limited proteolysis with Lys-C (red bars) or chymotrypsin (blue bars) are indicated.
(C) Segments of bRaf for which unique proteolytic peptides are identified in complex with Cdc37 are mapped in green on bRaf structure.
(D) Emission spectrum of ANS, in buffer (black) and in the presence of N-Cdc37 (red), Cdc37 (green), bRaf (pink), Cdc37-bRaf (cyan), and N-Cdc37-bRaf (blue).
Colored marks on the x axis correspond to the emission maximum of each spectrum (see also Figures S6 and S7).

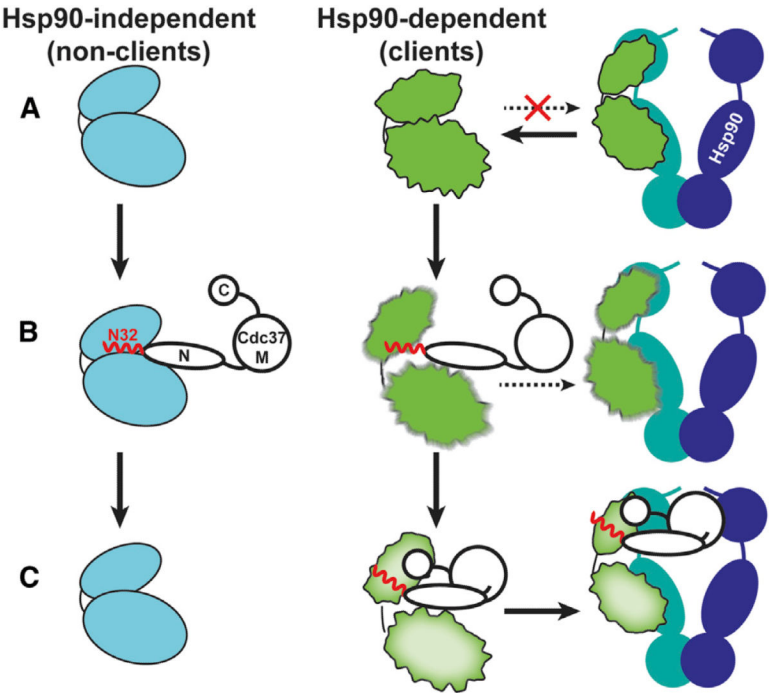

Figure 7. Cdc37-Mediated Kinase Recognition and Sorting

(A) Nonclients acquire a native conformation without assistance from Hsp90 and exhibit high thermodynamic stability (cyan bilobal structure). Clients exhibit a near-native conformation and low thermodynamic stability (rough bilobal structure shown in green), but do not associate with Hsp90. Cdc37 is shown in black outlines, the flexible N-terminal tail and the beginning of helix α_1 (N32) in red, and the Hsp90 dimer in blue/green.

(B) N-Cdc37, and particularly N32, recognizes both clients and nonclients, providing broad kinase family specificity. Binding of N-Cdc37 does not affect the conformational properties of nonclients but destabilizes the structure of clients. In vivo studies show that N-Cdc37 promotes kinase loading to Hsp90, but only inefficiently.

(C) Nonclients dissociate from Cdc37, while clients stably associate also with C-Cdc37, in a metastable conformation that is poised for efficient recruitment to Hsp90.